9-6-2018

Seniority Structure of $^{136}Xe_{82}$

Erin E. Peters
University of Kentucky, fe.peters@uky.edu

P. Van Isacker
Grand Accélérateur National d'Ions Lourd, France

Anagha Chakraborty
Siksha-Bhavana, India

Benjamin P. Crider
Mississippi State University

A. Kumar
Banaras Hindu University, India

See next page for additional authors

Seniority Structure of $^{136}\text{Xe}_{82}$

Authors

Erin E. Peters, P. Van Isacker, Anagha Chakraborty, Benjamin P. Crider, A. Kumar, S. H. Liu, Marcus T. McEllistrem, C. V. Mehl, Francisco M. Prados-Estévez, T. J. Ross, J. L. Wood, and Steven W. Yates

Seniority structure of ^{136}Xe$_{82}$

E. E. Peters,[1,*] P. Van Isacker,[2,†] A. Chakraborty,[1,3,†] B. P. Crider,[3,‡] A. Kumar,[1,3,§] S. H. Liu,[1,3] M. T. McEllistrem,[3]
C. V. Mehl,[4] F. M. Prados-Estévez,[1,3] T. J. Ross,[1,3] J. L. Wood,[5] and S. W. Yates[1,3,‖]

[1]*Department of Chemistry, University of Kentucky, Lexington, Kentucky 40506-0055, USA*
[2]*Grand Accélérateur National d'Ions Lourds, CEA/DRF-CNRS/IN2P3, Bd Henri Becquerel, F-14076 Caen, France*
[3]*Department of Physics and Astronomy, University of Kentucky, Lexington, Kentucky 40506-0055, USA*
[4]*Department of Physics, University of the Western Cape, P/BX17, ZA-7535, South Africa*
[5]*School of Physics, Georgia Institute of Technology, Atlanta, Georgia 30332, USA*

The level structure of the $N = 82$ nucleus ^{136}Xe was studied with the inelastic neutron scattering reaction followed by γ-ray detection. A number of the spins and parities were reassigned, and many level lifetimes were determined for the first time using the Doppler-shift attenuation method. New shell-model calculations were also performed using both the full $Z = 50$–82 model space, and a reduced model space including only the $1d_{5/2}$ and $0g_{7/2}$ orbitals. This new information characterizing ^{136}Xe was used to identify the seniority structure of the low-lying levels and to assign $(\pi 0g_{7/2})^4_{\upsilon=0}$, $(\pi 0g_{7/2})^4_{\upsilon=2}$, $(\pi 0g_{7/2})^4_{\upsilon=4}$, $(\pi 1d_{5/2})(\pi 0g_{7/2})^3_{\upsilon=1}$, and $(\pi 1d_{5/2})^2(\pi 0g_{7/2})^2_{\upsilon=0}$ configurations to describe all observed states below 2.8 MeV.

I. INTRODUCTION

The low-lying states in ^{136}Xe, with a closed $N = 82$ neutron shell and only four protons beyond the $Z = 50$ closed shell, should be well understood in terms of seniority structure. Seniority (υ) refers to the number of particles that are not in pairs coupled to angular momentum $J = 0$ [1]. The ground state of ^{136}Xe may be described by four protons residing in the $0g_{7/2}$ orbital as two pairs coupled to angular momentum $J = 0$, i.e., seniority $\upsilon = 0$. Excited states with configurations of one broken pair ($\upsilon = 2$) or two broken pairs ($\upsilon = 4$) should also exist. Multiplets arising from a single proton in the $1d_{5/2}$ orbital and three protons in the $0g_{7/2}$ orbital ($\upsilon = 1$ states) and two protons in each orbital ($\upsilon = 0$ states) are possible as well. Calculations using the generalized seniority scheme (GSS) [2], shell model [3,4], and the quasiparticle random phase approximation (QRPA) [5] have predicted the level energies of some of the multiplets produced, but they have not been definitively established experimentally.

In addition to being interesting from a structural point of view, ^{136}Xe plays a prominent role in ongoing searches for neutrinoless double-β decay ($0\nu\beta\beta$) as it is the candidate at the focus of experiments such as EXO-200 [6], NEXT [7], and KamLAND-Zen [8]. Comprehensive structural information provides crucial tests for nuclear structure models used in calculating the nuclear matrix element for $0\nu\beta\beta$ and the neutrino mass, if this exotic decay process is observed.

To obtain detailed spectroscopic information for ^{136}Xe, we studied this nucleus at the University of Kentucky Accelerator Laboratory (UKAL) using the inelastic neutron scattering (INS) reaction. For these measurements, highly enriched xenon gas was converted to solid ^{136}XeF$_2$ and γ-ray spectroscopic measurements were performed following INS with nearly monoenergetic neutrons. The excitation function and angular distribution measurements yielded branching ratios, multipole mixing ratios, and level lifetimes (from the Doppler-shift attenuation method [9]), which allowed the determination of reduced transition probabilities.

New shell-model calculations were also performed for ^{136}Xe. Two approaches were employed: one utilized the full $Z = 50$–82 model space, and another used a reduced model space involving only the $1d_{5/2}$ and $0g_{7/2}$ orbitals.

II. EXPERIMENTS

INS experiments were carried out at UKAL utilizing the 7 MV Van de Graaff accelerator to produce a pulsed (1.875 MHz in frequency) and bunched ($\approx$1 ns in width) proton beam. The protons impinged on a target of tritium gas to produce nearly monoenergetic ($\Delta E_n \approx 60$ keV) fast neutrons via the ^{3}H$(p, n)^3$He reaction. The scattering sample was 10.65 g of ^{136}XeF$_2$ converted from highly enriched (99.952% ^{136}Xe) xenon gas as described in Ref. [10]; the material was contained in a polytetrafluoroethylene vial with an inner diameter of 1.8 cm. The γ rays emitted in the reaction were detected with an $\approx$50% relative efficiency high-purity germanium (HPGe) detector surrounded by an annular bismuth germanate (BGO) detector, which served as both an active shield and Compton suppressor. Time-of-flight gating
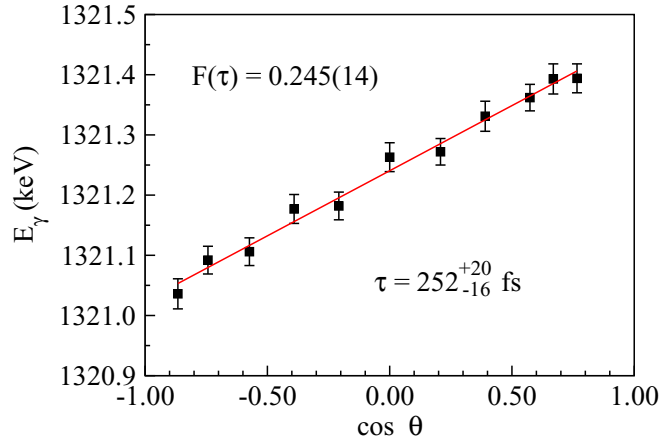
FIG. 1. Data for the determination of the lifetime of the 2634.3 keV level from the Doppler shift of the 1321.2 keV γ ray.

was also used to further reduce background contributions. Radioactive sources of ^{24}Na and ^{60}Co were used for online energy calibrations, while ^{226}Ra and ^{56}Co were used for offline efficiency and nonlinearity corrections.

Both excitation function and angular distribution data were obtained. Excitation function data were taken at a detection angle of 90° relative to the beam axis in 100 keV increments from 2.5 to 4.1 MeV incident neutron energies. These data afforded the placement of γ rays in the level scheme based on the observed neutron energy thresholds. The comparison of the γ-ray yields as a function of incident neutron energy with predicted cross sections from statistical model calculations using the code CINDY [11] aided in the determination of level spins. Angular distributions were performed by varying the detection angle in the range of 40° to 150° while holding the incident neutron energy constant at 3.2 or 3.8 MeV. From these data, transition multipolarities and mixing ratios were obtained, as well as level lifetimes from a few femtoseconds to about 2 ps using the Doppler-shift attenuation method [9]. Lifetimes were determined by comparison of the experimental attenuation factor, $F(\tau)$, describing the slowing-down process of the recoiling nucleus, with that calculated using the Winterbon formalism [12] as a function of the lifetime. $F(\tau)$ was extracted from the slope of the linear fit to the data according to the equation

$$E_\gamma(\theta) = E_0\Big[1 + F(\tau)\frac{v_{\text{c.m.}}}{c}\cos\theta\Big], \qquad (1)$$

where $E_\gamma(\theta)$ is the γ-ray energy as a function of the angle of detection with respect to the beam axis, E_0 is the energy of the γ ray emitted by the nucleus at rest, $v_{\text{c.m.}}$ is the recoil velocity of the center of mass, and c is the speed of light [9]. An example of the Doppler-shift data is shown in Fig. 1.

III. RESULTS

A summary of the data for levels in ^{136}Xe from the current experiments is provided in Table I. Comments on some of the levels to which these measurements have contributed uniquely are provided.

A. Level discussions

1. Previously known levels

1891.7 keV 6^+ state. Though there is definitive evidence of its presence, the lone 197.3 keV γ ray from this state is completely obscured by a γ ray from the ^{19}F$(n, n'\gamma)$ reaction and a background γ ray; fluorine is present in both the ^{136}XeF$_2$ sample and the polytetrafluoroethylene vial. The energy and spin of this level were taken from the Nuclear Data Sheets (NDS) [14].

2125.8 keV 4^+ state. The NDS [14] lists a spin-parity of $3^+, 4^+$, but we firmly establish this state as 4^+ based on the angular distribution data, especially that of the 812.7 keV γ ray to the 2_1^+ state.

2444.5 keV 5^+ state. A spin of 5 with no parity is given in the NDS [14] for this level, which was proposed as a potential 5^+ state by Mantica *et al.* [15] from β^- decay of ^{136}I. As the angular distributions of the 318.7, 552.8, and 750.1 keV γ rays agree with the spin-5 assignment and have measurable nonzero mixing ratios, these are transitions of mixed $E2/M1$ multipolarity, which establishes positive parity.

2465.1 keV 4^+ state. The NDS [14] assigns a tentative (4^+) spin for this level. Our angular distribution measurements indicate that the spin is either 4^+ or 6^+. As the level decays only to the 4_2^+ and 4_1^+ states and not to the 2^+ states, one might conclude that the spin is 6^+. However, our excitation function measurements show that the level cross section is too large to be consistent with a 6^+ spin, and compares better with that expected for a 4^+ level (see Fig. 2).

2560.0 keV 3^+ state. The NDS [14] compilation assigns a firm spin of 4^+ for this state, yet Mantica *et al.* [15] favored a spin of 3^+. Our angular distribution measurements, however, show dipole character for the 1246.9 keV γ ray, which is inconsistent with the expected quadrupole nature of a 4^+ to 2^+ transition (see Fig. 3). The angular distributions of each decay branch are consistent with a spin of 3 and exhibit nonzero mixing ratios; thus we conclude a spin-parity of 3^+.

2581.3 keV 0^+ state. Only the $E0$ decay to the ground state was previously observed [15], but we identify γ rays corresponding to transitions to the 2_1^+ and 2_2^+ states, both of which have isotropic angular distributions and are consistent with a spin-parity assignment of 0^+.

2608.6 keV 5^+ state. The angular distributions of each γ ray are in better agreement with a spin of 5^+ rather than the NDS-assigned [14] 4^+ spin. The lack of observed transitions to the 2^+ states may provide additional support for the higher spin assignment. We do not observe the previously known 164.1 keV γ ray [14] in the single-angle spectra, but it may be present in the all-angles-summed 3.8 MeV angular distribution spectrum.

2634.3 keV 1^+ level. In the NDS [14], a firm 2^+ spin assignment is given, but we rather favor a spin of 1 based on the lack of quadrupole character of the angular distribution for the ground-state transition. Mantica *et al.* [15] suspected positive parity for the state due to its intense β population, and we agree with that assessment. We do not observe the previously reported 219.3 keV γ ray [14] in the single-angle spectra, but it may be present in the all-angles-summed 3.8 MeV angular distribution spectrum.

TABLE I. Level scheme, branching ratios (B.R.), multipole mixing ratios, average experimental attenuation factors, level lifetimes, and transition probabilities for ^{136}Xe. When two mixing ratios for $E2/M1$ multipolarity are possible, the solution with the lowest χ^2 value is listed first; the signs for the values follow the convention of Krane and Steffen [13]. The final column is the reduced transition probability for either $M1$ or $E1$ multipolarity, as appropriate.

E_{level} (keV)	E_γ (keV)	J_i^π	J_f^π	B.R.	δ or mult.	$\bar{\text{F}}(\tau)$	τ (fs)	$B(E2)$ (W.u.)	$B(M1)/B(E1)$ $(\mu_N^2)/(\text{mW.u.})$
1313.078(8)	1313.077(8)	2_1^+	0_1^+	1	$E2$				
1694.437(10)	381.360(7)	4_1^+	2_1^+	1	$E2$				
1891.752(12)	197.316(7)[a]	6_1^{+} [a]	4_1^+	1	$E2$				
2125.788(10)	431.359(20)	4_2^+	4_1^+	0.186(5)	-0.356^{+65}_{-58}				
	812.712(8)		2_1^+	0.814(5)	$E2$				
2261.857(14)	370.108(8)	6_2^+	6_1^+	1	$+0.79^{+12}_{-11}$ -0.033^{+64}_{-62}				
2289.668(15)	976.572(20)	2_2^+	2_1^+	0.184(6)	$+2.22^{+55}_{-47}$ $+0.024^{+86}_{-87}$	0.143(16)	469^{+69}_{-55}	7.2^{+16}_{-17} 0.005^{+120}_{-5}	0.0040^{+27}_{-17} 0.00239^{+41}_{-40}
	2289.694(26)		0_1^+	0.816(6)	$E2$			0.543^{+77}_{-73}	
2414.702(46)	1101.591(98)	2_3^+	2_1^+	0.069(5)	-0.41^{+29}_{-53}	0.245(18)	245^{+22}_{-19}	0.5^{+14}_{-5}	0.0102^{+35}_{-48}
	2414.717(60)		0_1^+	0.931(5)	$E2$			0.909^{+82}_{-79}	
2444.509(15)	182.586(54)	5_1^+	6_2^+	0.059(9)					
	318.738(48)		4_2^+	0.075(9)	$+0.08^{+18}_{-17}$				
	552.802(50)		6_1^+	0.097(9)	-0.6^{+3}_{-13}				
	750.071(12)		4_1^+	0.769(12)	-0.5^{+67}_{-91} -1.60^{+27}_{-29}				
2465.129(22)	339.341(20)	4_3^+	4_2^+	0.104(5)					
	770.686(80)		4_1^+	0.896(5)					
2560.012(14)	270.403(50)	3_1^+	2_2^+	0.029(4)	$+0.21^{+50}_{-35}$	0.060(31)	1200^{+1300}_{-500}	14^{+180}_{-14}	0.068^{+59}_{-49}
	434.224(16)		4_2^+	0.183(6)	-0.098^{+82}_{-77} -4.3^{+12}_{-20}			1.9^{+77}_{-19} 190^{+130}_{-110}	0.107^{+68}_{-59} 0.006^{+11}_{-4}
	865.615(26)		4_1^+	0.178(6)	-0.060^{+91}_{-98} -5.2^{+17}_{-54}			0.02^{+22}_{-2} 5.9^{+40}_{-33}	0.0132^{+83}_{-73} 0.0005^{+12}_{-4}
	1246.895(26)		2_1^+	0.611(8)	-0.238^{+47}_{-53}			0.18^{+24}_{-13}	0.0144^{+90}_{-78}
2581.250(34)	291.582(30)	0_2^+	2_2^+	0.656(52)	$E2$				
	1267.84(48)		2_1^+	0.344(52)	$E2$				
2608.646(16)	346.799(16)	5_2^+	6_2^+	0.234(12)	-0.044^{+28}_{-35} -7.3^{+15}_{-18}				
	482.894(34)		4_2^+	0.284(17)	-0.13^{+11}_{-13} -4.7^{+21}_{-80}				
	716.86(12)		6_1^+	0.084(12)					
	914.175(22)		4_1^+	0.399(15)	$+0.58^{+15}_{-11}$ $+1.99^{+53}_{-47}$				
2634.318(16)	344.588(42)	1^+	2_2^+	0.110(10)		0.245(14)	252^{+20}_{-16}	1760(300)[b]	0.61(10)[b]
	1321.246(16)		2_1^+	0.679(66)				13.1(23)[b]	0.066(11)[b]
	2634.365(66)		0_1^+	0.210(20)	$M1$				0.00259^{+44}_{-42}
2849.590(23)	1536.510(22)	(0^+)	2_1^+	1	$(E2)$	0.203(51)	300^{+120}_{-70}	7.7^{+25}_{-22}	
2869.155(35)	309.201(50)	2_4^+	3_1^+	0.095(29)		0.223(21)	282^{+35}_{-31}	2300(1100)[b]	0.65(30)[b]
	1555.91(21)		2_1^+	0.074(22)				0.57(26)[b]	0.0040^{+18}_{-15}[b]
	2869.109(48)		0_1^+	0.83(25)	$E2$			0.30(14)	
2944.686(33)	682.837(34)	5_3^+	6_2^+	0.433(16)	$+0.53^{+12}_{-8}$ $+2.36^{+72}_{-54}$				
	1052.72(17)		6_1^+	0.135(12)	-0.31^{+19}_{-34} -2.3^{+11}_{-22}				
	1250.249(82)		4_1^+	0.433(18)					

TABLE I. (*Continued.*)

E_{level} (keV)	E_γ (keV)	J_i^π	J_f^π	B.R.	δ or mult.	$\bar{F}(\tau)$	τ (fs)	$B(E2)$ (W.u.)	$B(M1)/B(E1)$ $(\mu_N^2)/(mW.u.)$
2953.041(24)	827.238(74)	4_4^+	4_2^+	0.096(29)	$+2.9^{+34}_{-10}$	0.146(17)	467^{+73}_{-58}	9.3^{+58}_{-44}	0.0022^{+46}_{-18}
					-0.45^{+19}_{-23}			1.7^{+32}_{-14}	0.017^{+12}_{-9}
	1258.6(2)		4_1^+	0.53(16)				$7.1(34)^b$	0.033^{+16b}_{-13}
	1639.965(24)		2_1^+	0.37(11)	$E2$			1.32^{+64}_{-52}	
2979.108(24)	1666.041(26)	2_5^+	2_1^+	0.327(6)	-1.52^{+38}_{-52}	0.435(16)	108^{+7}_{-6}	3.23^{+80}_{-83}	0.0113^{+63}_{-46}
	2979.060(54)		0_1^+	0.673(6)	$E2$			0.522(36)	
3002.455(14)	1689.377(12)	$(2^+, 3^+)$	2_1^+	1		0.070(17)	1050^{+370}_{-220}		
3002.580(30)	1308.143(28)		4_1^+	1		0.113(30)	620^{+260}_{-140}		
3195.415(43)	1500.995(60)	2_6^+	4_1^+	0.176(5)	$E2$	0.147(23)	456^{+99}_{-73}	1.00^{+22}_{-20}	
	1882.28(18)		2_1^+	0.110(6)				$0.201(51)^b$	0.00206^{+53b}_{-46}
	3195.403(64)		0_1^+	0.714(7)	$E2$			0.092^{+19}_{-18}	
3211.916(62)	362.28(12)	1	(0^+)	0.103(28)		0.136(35)	490^{+200}_{-110}		
	922.26(15)		2_2^+	0.129(38)					
	3211.938(82)		0_1^+	0.77(11)					
3224.387(26)	1529.925(34)	(4^+)	4_1^+	0.391(7)	-0.81^{+11}_{-13}	0.188(18)	341^{+44}_{-37}	1.07^{+37}_{-30}	0.0110^{+30}_{-25}
	1911.337(36)		2_1^+	0.609(7)	$E2$			1.38^{+19}_{-17}	
3275.284(33)	1962.206(32)	3^-	2_1^+	1	$E1$	0.698(21)	37^{+4}_{-3}		1.32^{+12}_{-13}
3322.768(33)	2009.690(32)	4^+	2_1^+	1	$E2$	0.345(21)	152^{+15}_{-13}	3.94^{+37}_{-35}	
3340.958(56)	926.260(80)	3^+	2_3^+	0.361(18)	-0.20^{+12}_{-14}				
					-2.6^{+8}_{-13}				
	1646.47(11)		4_1^+	0.197(12)	$+1.13^{+69}_{-40}$				
	2027.908(86)		2_1^+	0.442(18)	$+0.28^{+12}_{-11}$				
3349.410(64)	1654.97(14)	2_7^+	4_1^+	0.088(8)	$E2$	0.385(28)	128^{+16}_{-14}	1.09^{+25}_{-21}	
	2036.20(21)		2_1^+	0.098(10)	-1.5^{+8}_{-24}			0.29^{+21}_{-18}	0.0016^{+26}_{-14}
	3349.429(76)		0_1^+	0.814(13)	$E2$			0.296^{+42}_{-37}	
3428.86(12)	1303.28(18)	(5^+)	4_2^+	0.585(26)					
	1734.29(15)		4_1^+	0.415(26)	-2.7^{+9}_{-15}				
					-0.36^{+16}_{-27}				
3526.05(11)	2212.97(11)		2_1^+	1					
3626.64(19)	2313.50(33)	2^+	2_1^+	0.246(26)		0.821(50)	19^{+7}_{-6}	$3.84(24)^b$	0.060^{+37b}_{-21}
	3626.68(24)		0_1^+	0.754(26)	$E2$			1.24^{+64}_{-37}	
3675.07(45)	3675.07(45)	2^+	0_1^+	1	$E2$	0.587(89)	57^{+24}_{-18}	0.51^{+24}_{-12}	

[a]From Ref. [14]. Information for this level could not be obtained due to contamination of the 197.3 keV γ ray from the ^{19}F$(n, n'\gamma)$ reaction, as well as a background γ ray. Fluorine is present in both the ^{136}XeF$_2$ sample and the polytetrafluoroethylene vial.
[b]Calculated assuming pure $E2$ or $M1$ multipolarity.

2849.6 keV (0^+) level. In previous β^--decay measurements, a ground-state transition from this level was observed [17]; however, we find no evidence of such a γ ray, even when summing the spectra for all of the angles in the angular distribution data set to increase the statistics. We only observe the 1536.5 keV γ ray with an isotropic angular distribution and thus conclude a tentative spin assignment of 0^+. The small cross section measured in the excitation function is also consistent with that expected for a 0^+ level.

2869.2 keV 2^+ state. The NDS [14] lists a spin-parity of $2^{(+)}$ for this state, yet the conclusion from photon scattering experiments [18] was a spin of 1. Based on the observation of the γ ray to the ground state with a quadrupole angular distribution (see Fig. 4), we confirm the 2^+ assignment. The 1555.9 keV γ ray is contaminated by a significantly Doppler-broadened γ ray from ^{19}F at all angles. The branching ratios were obtained by using the previously published γ-ray cross-section data obtained for ^{134}Xe and ^{136}Xe [16]. The spectra were taken at 125° to minimize the angular distribution effects and were taken sequentially for each scattering sample. By normalizing the spectra and subtracting the ^{134}Xe spectrum from the ^{136}Xe spectrum, the ^{19}F contribution may be removed, leaving only the contribution from ^{136}Xe in the 1556 keV region. The large uncertainties associated with the branching ratios reflect this additional manipulation of the data.
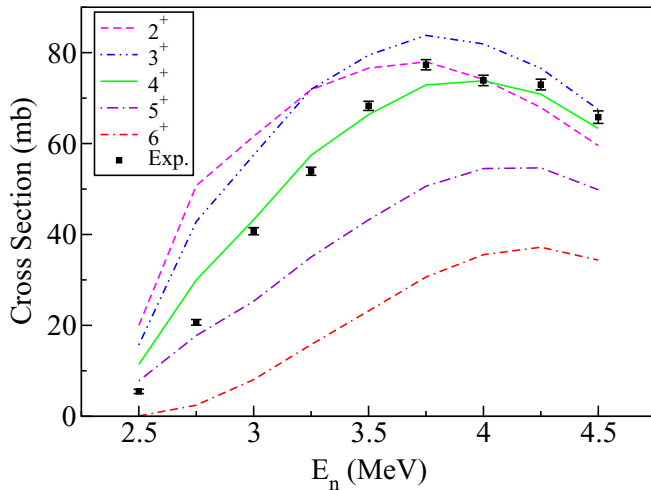
FIG. 2. Excitation function compared with CINDY calculations for various spins for the 2465.1 keV level. The data shown are from the measurements described in Ref. [16].

3211.9 keV 1 level. We observe a new 922.3 keV branch to the 2_2^+ state. The NDS [14] assigns a spin of 1, $2^{(+)}$, but we can confirm the spin is 1 by the dipole character of the angular distribution of the ground-state γ ray. We cannot, however, establish the parity.

3349.4 keV 2^+ state. Previously only observed in photon scattering experiments [18], the spin was tentatively assigned as $(1, 2^+)$. The spin-parity of this level is now assigned firmly as 2^+ based on the observation of a ground-state γ ray with a quadrupole angular distribution. Additional branches to the 2_1^+ and 4_1^+ states are also observed.

3626.7 keV 2^+ state. This state was previously observed only in photon scattering measurements [18,19]; one study concluded a spin of 1 [18], while the other assigned 1, 2^+ [19]. A ground-state γ ray with a quadrupole angular distribution and a γ ray to the 2_1^+ state are observed, thus confirming a spin-parity of 2^+. The branching ratios for this new level
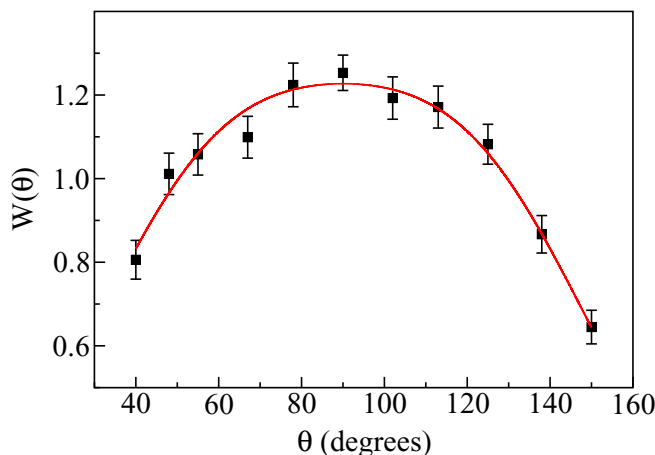

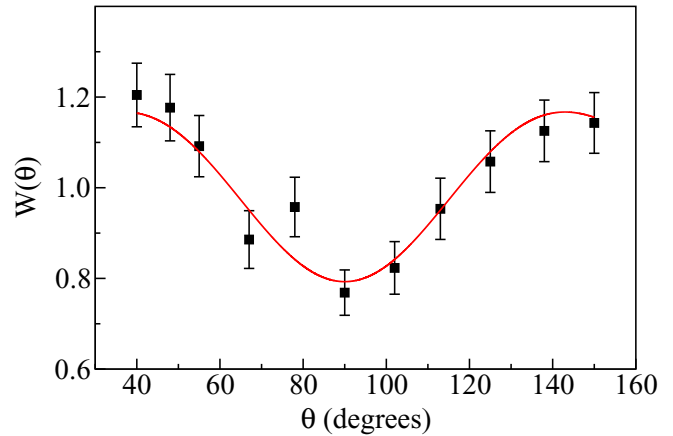FIG. 3. Angular distribution of the 1246.9 keV γ ray from the 2560.0 keV level.

FIG. 4. Angular distribution of the 2869.2 keV ground-state γ ray from a level of the same energy exhibiting quadrupole character.

were extracted from the all-angles-summed 3.8 MeV angular distribution spectrum due to the weak intensities of the γ rays.

3675.1 keV 2^+ state. Only a ground-state transition with a quadrupole angular distribution is observed. This γ ray was also observed in photon scattering experiments [18].

2. Newly observed levels

2944.7 keV 5^+ state. This state is a newly observed level with transitions to the 6_2^+, 6_1^+, and 4_1^+ states. The γ-ray angular distributions agree with a spin of 5 and exhibit nonzero mixing ratios, indicating $E2/M1$ multipolarity and thus positive parity.

2953.0 keV 4^+ state. γ rays were observed to decay from this level to the 4_2^+, 4_1^+, and 2_1^+ states. From the 1640.0 keV γ ray, we assign a 4^+ spin. The 1259 keV γ ray is contaminated by a considerably Doppler-broadened ^{19}F γ ray at all angles. As previously described for the 2869.2 keV level, the cross-section data were used to determine the branching ratios.

3002.5 and 3002.6 keV levels. These two levels are separated based on γ-ray energies and the difference in the lifetimes.

3195.4 keV 2^+ state. The spin of this level is assigned based on the observation of a ground-state γ ray with a quadrupole angular distribution. Additional branches to the 2_1^+ and 4_1^+ states are also observed.

3224.4 keV (4^+) level. From this level, only γ rays to the 4_1^+ and 2_1^+ states are established. We assign a tentative (4^+) spin and parity.

3322.8 keV 4^+ state. Decay branches to the 2_2^+ and 2_1^+ states with angular distributions consistent with a spin of 4 and pure $E2$ multipolarity are observed. We, therefore, assign a spin-parity of 4^+.

3341.0 keV 3^+ state. Each of the observed γ rays to the 2_3^+, 2_1^+, and 4_1^+ states exhibit angular distributions consistent with spin 3 and have measurable mixing ratios indicating mixed $E2/M1$ multipolarity and positive parity.

3428.9 keV (5^+) level. γ rays representing transitions to the 4_1^+ and 4_2^+ states are observed. The angular distributions of both are in agreement with a spin of 5^+. The branching ratios for this new level were extracted from the
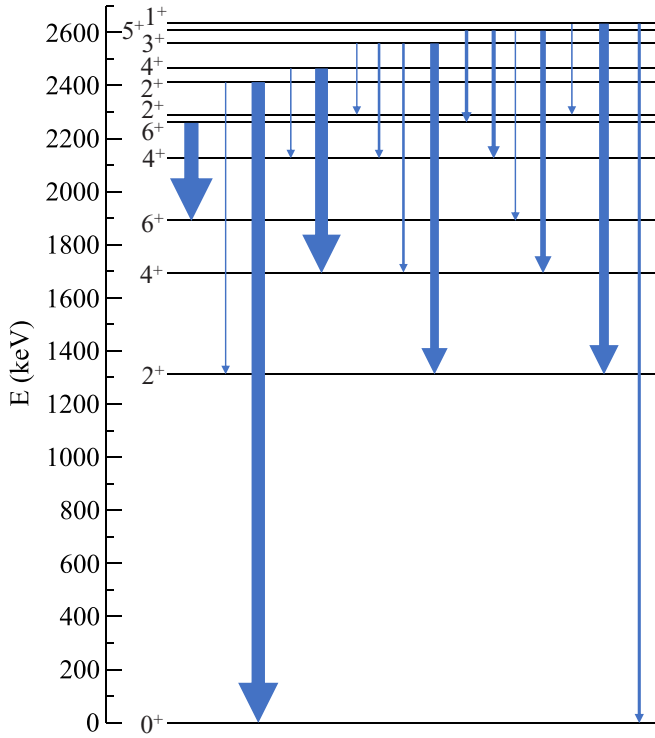
FIG. 5. Decays of the states with a dominant $\pi 1d_{5/2}(\pi 0g_{7/2})^3_{\upsilon=1}$ configuration. The arrow widths are representative of the branching ratios of the decays of each level.

all-angles-summed 3.8 MeV angular distribution spectrum due to the weak intensities of the γ rays.

3526.1 keV level. This level is placed based on a single 2213.0 keV γ ray with a 3.6 MeV threshold. The small intensity of the γ ray does not permit a spin assignment.

B. Configuration assignments of the states

The $(\pi 0g_{7/2})^4$ configuration with seniorities $\upsilon = 0$ and 2 gives rise to a state with $J^\pi = 0^+$ and a multiplet with $J^\pi = 2^+, 4^+, 6^+$ in order of increasing energy. These excitations are easily attributed to the ground, 2_1^+, 4_1^+, and 6_1^+ states, respectively.

The $\pi 1d_{5/2}(\pi 0g_{7/2})^3_{\upsilon=1}$ configuration produces a $J^\pi = 1^+, 2^+, 3^+, 4^+, 5^+, 6^+$ multiplet, where the odd-spin states are nearly degenerate and highest in energy, and the even-spin states are in order of decreasing energy with increasing spin. Assigning states with this configuration depends most upon the observed decays of the levels. Figure 5 shows the decay patterns of the states where the arrow widths represent the branching ratios; many of the level lifetimes are still unknown, thus the $B(E2)$ values cannot be compared. The 6_2^+ state at 2261.8 keV decays only to the 6_1^+ state and not to the 4_1^+ state. The 4_3^+ state at 2465.1 keV has a similar decay pattern in that only branches to the lower-lying 4^+ states, but not to any 2^+ states, are observed. The 6_2^+ and 4_3^+ states are thus thought to have a $\pi 1d_{5/2}(\pi 0g_{7/2})^3_{\upsilon=1}$ configuration. Similarly, the 2608.6 keV level is assigned as the 5^+ member because stronger decay branches to the 6_2^+ and 4_2^+ states are observed than for the 5_1^+ state. In addition, the 2608.6 keV state is
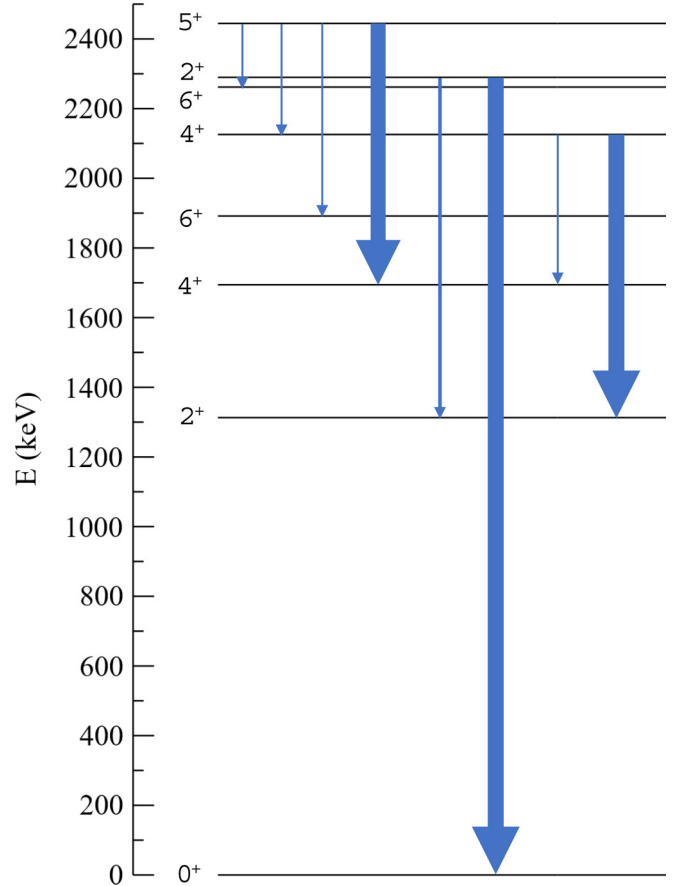

FIG. 6. Decays of the states with a dominant $(\pi 0g_{7/2})^4_{\upsilon=4}$ configuration. The arrow widths are representative of the branching ratios of the decays of each level.

nearest in energy to the easily assigned 1^+ and 3^+ members of the multiplet at 2634.3 and 2560.0 keV, respectively, as there is only one choice for each below 3 MeV. Finally, the 2_3^+ state is chosen as the remaining member of the multiplet based on its energy.

The $(\pi 0g_{7/2})^4_{\upsilon=4}$ configuration gives rise to a $J^\pi = 2^+, 4^+, 5^+, 8^+$ multiplet. We propose the 2289.7, 2125.8, and 2444.5 keV states as the 2^+, 4^+, and 5^+ members, respectively. These states all decay entirely or most strongly (largest branching ratios) to the $(\pi 0g_{7/2})^4_{\upsilon=0,2}$ states as shown in Fig. 6. We do not observe an 8^+ state as levels with $J > 6$ are very weakly populated in the INS reaction, but candidates exist from other measurements. A 2867 keV (8^+) state was observed in the decays of ^{248}Cm fission products and was tentatively assigned a $(\pi 0g_{7/2})^4_{\upsilon=4}$ configuration [20].

The $(\pi 1d_{5/2})^2(\pi 0g_{7/2})^2_{\upsilon=0}$ configuration produces a $J^\pi = 0^+, 2^+, 4^+$ multiplet in order of increasing energy. Here, we assign only the 2581.3 keV state as the 0^+ member of the multiplet. States with angular momentum 2^+ and 4^+ are found in the energy region near 3 MeV, but sufficient evidence is not present to distinguish them specifically as members of the multiplet for this configuration.

These proposed configuration assignments describe all states observed below 2.8 MeV in ^{136}Xe.

TABLE II. Comparison of the $B(E2)$ values determined in this work with those obtained from Coulomb excitation [25].

Transition	$B(E2; 2_i^+ \rightarrow 0_1^+)$ (W.u.)	
	Ref. [25]	Present work
$2_2^+ \rightarrow 0_1^+$	0.623^{+41}_{-32}	0.543^{+77}_{-73}
$2_3^+ \rightarrow 0_1^+$	$0.91(6)$	0.909^{+82}_{-79}
$2_4^+ \rightarrow 0_1^+$	0.234^{+50}_{-60}	$0.30(14)$
$2_5^+ \rightarrow 0_1^+$	$0.695(76)$	$0.522(36)$

IV. DISCUSSION

After the completion of our analysis, we became aware of the theoretical work by Isakov *et al.* [21] including both shell-model and QRPA calculations. Also in that paper are comparisons with experimental data found in the dissertation of Aas [22] that remain unpublished elsewhere and are not included in the NDS compilation [14]. In Aas's work [22], ^{136}I decay experiments were performed at Studsvik, Sweden; γ-γ coincidence data and lifetimes from fast-timing measurements were obtained. Included in the dissertation [22] is a comparison of the data with semiempirical shell-model calculations by Blomqvist [23], who used single-particle energies and two-body interaction matrix elements from the experimental excitation energies of ^{133}Sb and ^{134}Te and reported excellent agreement with the experimental levels of ^{136}Xe, i.e., a root-mean-square deviation of only 26 keV for states up to 2.8 MeV. However, there is at least the appearance of a symbiotic interaction between theory and experiment in this case. In the dissertation [22], it is stated that spin assignments for a few of the levels were made by considering those suggested in Ref. [23], yet Blomqvist compares with experimental data of unreferenced origin that are not compatible with the NDS compilation at the time [24], but are in agreement with Aas's dissertation [22]. We do, however, find excellent agreement between our experimentally derived spin-parity assignments and those presented by Aas [22].

Even more recently, we learned of unpublished Coulomb excitation data for ^{136}Xe found only in a dissertation by Stahl [25], which was obtained at the Legnaro National Laboratory using the AGATA demonstrator. These data afford a direct comparison between the $B(E2)$ values for $2_i^+ \rightarrow 0_1^+$ transitions from the Coulomb excitation measurements and our work as presented in Table II. The $B(E2)$ values are found to be in good agreement overall. Also noteworthy is the absence of the population in Coulomb excitation of the 2634.3 and 2849.6 keV levels, which are given spin-parities of 2^+ in the NDS [14], but we have reassigned them as $J^\pi = 1^+$ and (0^+), respectively.

As our work establishes many levels and transitions that are not calculated in the previous theoretical studies of ^{136}Xe [21–23], we present here new shell-model calculations for this isotope. Two approaches were followed. In the first, the full 50–82 model space was considered for the four protons, with single-particle energies and two-body matrix elements (TBMEs) taken from Ref. [26], referred to as N82K. This approach is similar in spirit to the calculation of Blomqvist [23].
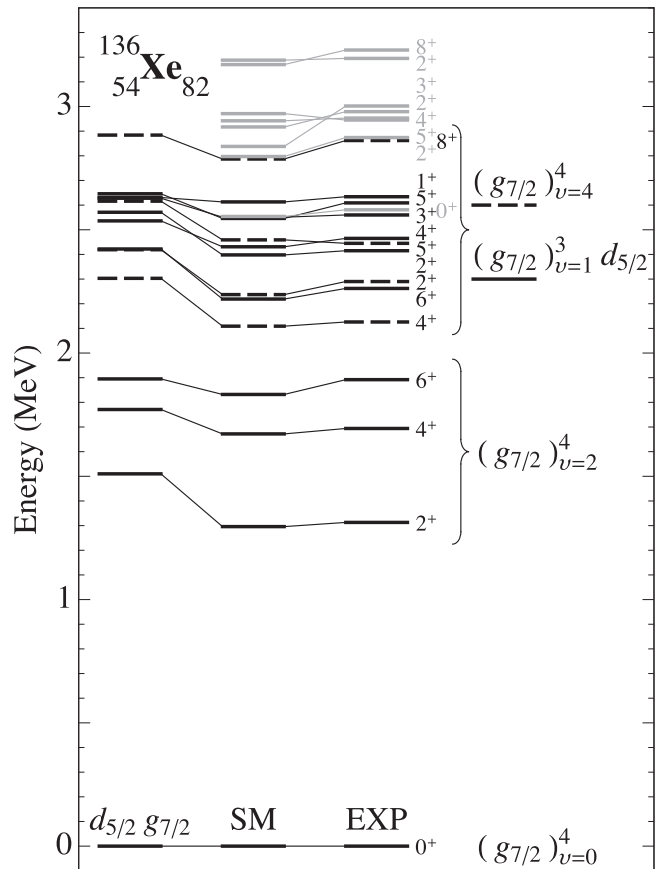

FIG. 7. The observed levels in ^{136}Xe ("EXP") compared with a two-orbital calculation "$d_{5/2}g_{7/2}$" and a full 50–82 shell-model calculation ("SM"). The proposed seniority structure of the levels is indicated on the right: $(\pi 0g_{7/2})^4$ with $\upsilon = 0$, $(\pi 0g_{7/2})^4$ with $\upsilon = 2$, $(\pi 0g_{7/2})^4$ with $\upsilon = 4$, and $(\pi 0g_{7/2})^3$ with $\upsilon = 1$ coupled to $\pi 1d_{5/2}$. Additional levels are indicated in gray.

In the second approach, the model space was reduced to the $1d_{5/2}$ and $0g_{7/2}$ orbitals, akin to the study of Isakov *et al.* [21].

The resulting levels are shown in Fig. 7. The left column, labeled "$d_{5/2}g_{7/2}$," shows the levels obtained in the restricted shell-model space. It should be noted that reasonable results can only be obtained with an effective interaction that is constructed specifically for that space. Some of the TBMEs in the $d_{5/2}g_{7/2}$ space can be determined empirically from the levels of ^{134}Te. In particular, the diagonal matrix elements involving $|(0g_{7/2})^2; J\rangle$, with coupled angular momenta $J = 0, 2, 4, 6$, and $|0g_{7/2}1d_{5/2}; J\rangle$, with $J = 1, 2, 3, 4, 5, 6$, were determined from data. Other matrix elements are of lesser importance and were taken from Ref. [26].

Some insight into the structure of the low-lying levels can be obtained from this calculation. The ground state corresponds dominantly to four protons in $0g_{7/2}$ with seniority $\upsilon = 0$, that is, for two pairs coupled to angular momentum $J = 0$ [1]. In addition, the four protons in the $0g_{7/2}$ orbital give rise to a multiplet with $\upsilon = 2$ (one broken pair) and a multiplet with $\upsilon = 4$ (two broken pairs). Furthermore, the multiplet with one proton excited into the $1d_{5/2}$ orbital coupled to three protons in $0g_{7/2}$ with seniority $\upsilon = 1$, leading to the angular

TABLE III. Observed (EXP) and calculated ($d_{5/2}g_{7/2}$ and SM) $B(E2)$ and $B(M1)$ values in ^{136}Xe. In the case of $E2/M1$ mixing, the quoted experimental values are obtained from the mixing ratio with the smallest χ^2 value. See text for details on the calculations.

Transition	$B(E2; J_i \rightarrow J_f)$ (W.u.)			$B(M1; J_i \rightarrow J_f)$ (μ_N^2)		
	EXP	$d_{5/2}g_{7/2}$	SM	EXP	$d_{5/2}g_{7/2}$	SM ($q = 0.7$)
$2_1^+ \rightarrow 0_1^+$	$16.6(24)^{a,b}$	$\frac{605}{63\pi}e_\pi^2$	9.63			
$4_1^+ \rightarrow 2_1^+$	$1.281(17)^a$	0	2.07			
$6_1^+ \rightarrow 4_1^+$	$0.0132(4)^a$	0	0.003			
$2_2^+ \rightarrow 0_1^+$	0.543^{+77}_{-73}	0	0.29			
$2_3^+ \rightarrow 0_1^+$	0.909^{+82}_{-79}	$\frac{18}{35\pi}e_\pi^2$	0.30			
$2_4^+ \rightarrow 0_1^+$	$0.30(14)$		0.23			
$2_5^+ \rightarrow 0_1^+$	$0.522(36)$		0.54			
$2_2^+ \rightarrow 2_1^+$	7.2^{+16}_{-17}	$\frac{6655}{686\pi}e_\pi^2$	2.49	0.0040^{+27}_{-17}	0	0.012
$2_3^+ \rightarrow 2_1^+$	0.5^{+14}_{-5}	$\frac{5}{343\pi}e_\pi^2$	2.82	0.0102^{+35}_{-48}	0	0.017
$3_1^+ \rightarrow 2_1^+$	0.18^{+24}_{-13}	$\frac{100}{343\pi}e_\pi^2$	0.042	0.0144^{+90}_{-78}	0	0.0010
$3_1^+ \rightarrow 2_2^+$	14^{+180}_{-14}	0	0.68	0.068^{+59}_{-49}	0	0.20
$3_1^+ \rightarrow 2_3^+$		$\frac{3872}{27783\pi}e_\pi^2$	0.064		$\frac{112}{405\pi}(g_l^\pi - g_s^\pi)^2$	0.37
$3_1^+ \rightarrow 4_1^+$	0.02^{+22}_{-2}	$\frac{22}{1029\pi}e_\pi^2$	0.23	0.0132^{+83}_{-73}	0	0.061
$3_1^+ \rightarrow 4_2^+$	1.9^{+77}_{-19}	0	0.014	0.107^{+68}_{-59}	0	0.0001
$3_1^+ \rightarrow 4_3^+$		$\frac{3738779}{8890560\pi}e_\pi^2$	0.50		$\frac{77}{240\pi}(g_l^\pi - g_s^\pi)^2$	0.57
$1^+ \rightarrow 2_1^+$	$13.1(23)^c$	$\frac{25}{49\pi}e_\pi^2$	0.15	$0.066(11)^c$	0	0.13
$1^+ \rightarrow 2_2^+$	$1760(300)^c$	0	0.29	$0.61(10)^c$	0	0.58
$1^+ \rightarrow 2_3^+$		$\frac{755161}{127008\pi}e_\pi^2$	0.76		$\frac{49}{120\pi}(g_l^\pi - g_s^\pi)^2$	0.46
$1^+ \rightarrow 0_1^+$				0.00259^{+44}_{-42}	0	0.0001

[a]From Ref. [14].
[b]Other more recently measured values include 10.3(4) W.u. [27] and 9.60^{+43}_{-49} W.u. [25].
[c]Assuming pure $E2$ or $M1$ multipolarity.

momenta $J = 1$–6, is also present. All of these levels are found in ^{136}Xe (see column "EXP" of Fig. 7), which shows all levels of Table I that have a firm spin-parity assignment. The middle column ("SM") of Fig. 7 shows the results of the shell model in the 50–82 space with the N82K interaction. This calculation confirms the aforementioned seniority structure of the low-lying levels, albeit with large admixtures of the other orbitals. For example, the ground state is found to be 59% $(0g_{7/2})^4_{\nu=0}$. The association between the "$d_{5/2}g_{7/2}$" and "SM" levels in Fig. 7 is therefore made on the basis of dominant wave-function components with a certain seniority structure. In addition, the full shell model is able to reproduce rather accurately the higher-lying levels (shown in gray).

While energies are satisfactorily described in the shell model, such cannot be said of the $E2$ and $M1$ strength observed in this work. The results are shown in Table III, which lists the measured values, the analytic results in the case of the simplified configurations of Fig. 7 labeled "$d_{5/2}g_{7/2}$", and the results obtained with the N82K interaction in the 50–82 model space labeled "SM". The $B(E2)$ values are obtained with an effective charge of the proton of $e_\pi = 1.73e$, leading to $B(E2; 2_1^+ \rightarrow 0_1^+) \approx 10$ W.u., which is a plausible value in view of the different recent measurements. It is seen that very large and erratic discrepancies occur between theory and experiment. The same situation is found for the $M1$ strength. The $B(M1)$ values are calculated with an effective $M1$ operator, which in principle includes an orbital, a spin, and a tensor term with corresponding g factors, g_l^π, g_s^π, and

g_t^π, respectively. The tensor term provides a small correction, which usually is neglected, $g_t^\pi = 0$, while the orbital g factor usually does not deviate strongly from its free value, $g_l^\pi = 1$. Most shell-model studies therefore introduce an effective $M1$ operator by "quenching" its spin part by a certain factor q. The explicit dependence on the orbital and spin g factors is shown in Table III for the few nonzero $M1$ transitions in the analytic calculation. It would have been a miracle if a single value of q were able to reproduce all observed $B(M1)$ values, and, of course, the miracle does not happen.

V. CONCLUSIONS

The inelastic neutron scattering reaction was employed to study the level structure of ^{136}Xe. Many level lifetimes were measured for the first time with the Doppler-shift attenuation method and the low-lying excited states were characterized. New information on the spins and parities and the decays of the states was used to assign seniority configurations to describe all observed states below 2.8 MeV in ^{136}Xe.

Excellent agreement is found between the observed energies of ^{136}Xe and the shell-model calculation with the N82K interaction in the full 50–82 space. The shell-model calculation in the restricted space, consisting of only the $1d_{5/2}$ and $0g_{7/2}$ orbitals, adequately describes the energies of the low-lying levels of this isotope. The two results are obtained with different interactions that are constructed for the specific model space under consideration. At the same time, the

shell-model calculation in the full 50–82 space fails to reproduce the observed $E2$ and $M1$ strengths in ^{136}Xe. An analysis of the structure of the calculated $B(M1)$ values reveals the crucial role of the quenching factor of the spin part of the $M1$ operator. The use of a single quenching factor q for all $M1$ transitions (or, for that matter, a single effective charge for all $E2$ transitions) is probably too crude an approximation. This failing suggests that more sophisticated effective operators are needed for the calculation of electromagnetic-transition properties in the shell model.

[1] I. Talmi, *Simple Models of Complex Nuclei: The Shell Model and the Interacting Boson Model* (Harwood, Chur, 1993).

[2] O. Scholten and H. Kruse, Phys. Lett. B **125**, 113 (1983).

[3] A. Holt, T. Engeland, E. Osnes, M. Hjorth-Jensen, and J. Suhonen, Nucl. Phys. A **618**, 107 (1997).

[4] K. Higashiyama, N. Yoshinaga, and K. Tanabe, Phys. Rev. C **65**, 054317 (2002).

[5] K. I. Erokhina, V. I. Isakov, B. Fogelberg, and H. Mach, Phys. Part. Nuclei Lett. **4**, 5 (2001).

[6] M. Auger, D. J. Auty, P. S. Barbeau, E. Beauchamp, V. Belov, C. Benitez-Medina, M. Breidenbach, T. Brunner, A. Burenkov, B. Cleveland, S. Cook, T. Daniels, M. Danilov, C. G. Davis, S. Delaquis, R. deVoe, A. Dobi, M. J. Dolinski, A. Dolgolenko, M. Dunford, W. Fairbank, J. Farine, W. Feldmeier, P. Fierlinger, D. Franco, G. Giroux, R. Gornea, K. Graham, G. Gratta, C. Hall, K. Hall, C. Hargrove, S. Herrin, M. Hughes, A. Johnson, T. N. Johnson, A. Karelin, L. J. Kaufman, A. Kuchenkov, K. S. Kumar, D. S. Leonard, F. Leonard, D. Mackay, R. MacLellan, M. Marino, B. Mong, M. Montero Díez, A. R. Müller, R. Neilson, R. Nelson, A. Odian, I. Ostrovskiy, K. O'Sullivan, C. Ouellet, A. Piepke, A. Pocar, C. Y. Prescott, K. Pushkin, P. C. Rowson, J. J. Russell, A. Sabourov, D. Sinclair, S. Slutsky, V. Stekhanov, T. Tolba, D. Tosi, K. Twelker, P. Vogel, J.-L. Vuilleumier, A. Waite, T. Walton, M. Weber, U. Wichoski, J. Wodin, J. D. Wright, L. Yang, Y.-R. Yen, and O. Y. Zeldovich (EXO-200 Collaboration), Phys. Rev. Lett. **109**, 032505 (2012).

[7] J. Martín-Albo, J. Muñoz Vidal, P. Ferrario, M. Nebot-Guinot, J. J. Gómez-Cadenas, V. Álvarez, C. D. R. Azevedo, F. I. G. Borges, S. Cárcel, J. V. Carrión, S. Cebrián, A. Cervera, C. A. N. Conde, J. Díaz, M. Diesburg, R. Esteve, L. M. P. Fernandes, A. L. Ferreira, E. D. C. Freitas, A. Goldschmidt, D. González-Díaz, R. M. Gutiérrez, J. Hauptman, C. A. O. Henriques, J. A. Hernando Morata, V. Herrero, L. Labarga, A. Laing, P. Lebrun, I. Liubarsky, N. López-March, D. Lorca, M. Losada, G. Martínez-Lema, A. Martínez, F. Monrabal, C. M. B. Monteiro, F. J. Mora, L. M. Moutinho, P. Novella, D. Nygren, B. Palmeiro, A. Para, M. Querol, J. Renner, L. Ripoll, J. Rodríguez, F. P. Santos, J. M. F. dos Santos, L. Serra, D. Shuman, A. Simón, C. Sofka, M. Sorel, T. Stiegler, J. F. Toledo, J. Torrent, Z. Tsamalaidze, J. F. C. A. Veloso, R. Webb, J. T. White, N. Yahlali, and H. Yepes-Ramírez, J. High Energy Phys. 05 (2016) 159.

[8] A. Gando, Y. Gando, T. Hachiya, A. Hayashi, S. Hayashida, H. Ikeda, K. Inoue, K. Ishidoshiro, Y. Karino, M. Koga, S. Matsuda, T. Mitsui, K. Nakamura, S. Obara, T. Oura, H. Ozaki, I. Shimizu, Y. Shirahata, J. Shirai, A. Suzuki, T. Takai, K. Tamae, K. Teraoka, K. Ueshima, H. Watanabe, A. Kozlov, Y. Takemoto, S. Yoshida, K. Fushimi, T. I. Banks, B. E. Berger,

B. K. Fujikawa, T. O'Donnell, L. A. Winslow, Y. Efremenko, H. J. Karwowski, D. M. Markoff, W. Tornow, J. A. Detwiler, S. Enomoto, and M. P. Decowski (KamLAND-Zen Collaboration), Phys. Rev. Lett. **117**, 082503 (2016).

[9] T. Belgya, G. Molnár, and S. W. Yates, Nucl. Phys. A **607**, 43 (1996).

[10] E. E. Peters, T. J. Ross, S. F. Ashley, A. Chakraborty, B. P. Crider, M. D. Hennek, S. H. Liu, M. T. McEllistrem, S. Mukhopadhyay, F. M. Prados-Estévez, A. P. D. Ramirez, J. S. Thrasher, and S. W. Yates, Phys. Rev. C **94**, 024313 (2016).

[11] E. Sheldon and V. C. Rogers, Comput. Phys. Commun. **6**, 99 (1973).

[12] K. B. Winterbon, Nucl. Phys. A **246**, 293 (1975).

[13] K. S. Krane and R. M. Steffen, Phys. Rev. C **2**, 724 (1970).

[14] A. Sonzogni, Nucl. Data Sheets **95**, 837 (2002).

[15] P. F. Mantica, B. E. Zimmerman, W. B. Walters, and K. Heyde, Phys. Rev. C **43**, 1696 (1991).

[16] E. E. Peters, T. J. Ross, S. H. Liu, M. T. McEllistrem, and S. W. Yates, Phys. Rev. C **95**, 014325 (2017).

[17] W. R. Western, J. C. Hill, W. L. Talbert, and W. C. Schick, Phys. Rev. C **15**, 1822 (1977).

[18] H. von Garrel, P. von Bretano, C. Fransen, G. Friessner, N. Hollmann, J. Jolie, F. Käppeler, L. Käubler, U. Kneissl, C. Kohstall, L. Kostov, A. Linnemann, D. Mücher, N. Pietralla, H. H. Pitz, G. Rusev, M. Scheck, K. D. Schilling, C. Scholl, R. Schwengner, F. Stedile, S. Walter, V. Werner, and K. Wisshak, Phys. Rev. C **73**, 054315 (2006).

[19] D. Savran, M. Elvers, J. Endres, M. Fritzsche, B. Löher, N. Pietralla, V. Y. Ponomarev, C. Romig, L. Schnorrenberger, K. Sonnabend, and A. Zilges, Phys. Rev. C **84**, 024326 (2011).

[20] P. J. Daly, P. Bhattacharyya, C. T. Zhang, Z. W. Grabowski, R. Broda, B. Fornal, I. Ahmad, T. Lauritsen, L. R. Morss, W. Urban, W. R. Phillips, J. L. Durell, M. J. Leddy, A. G. Smith, B. J. Varley, N. Schulz, E. Lubkiewicz, M. Bentaleb, and J. Blomqvist, Phys. Rev. C **59**, 3066 (1999).

[21] V. I. Isakov, H. Mach, B. Fogelberg, K. I. Erokhina, A. J. Aas, and E. Hagebø, Phys. At. Nucl. **68**, 1487 (2005).

[22] A. J. Aas, Ph.D. thesis, University of Oslo, Norway, 1999 (unpublished).

[23] J. Blomqvist, Acta Phys. Pol. **B30**, 697 (1999).

[24] J. K. Tuli, Nucl. Data Sheets **71**, 1 (1994).

[25] C. Stahl, Master's thesis, Technical University of Darmstadt, Germany, 2015 (unpublished).

[26] H. Kruse and B. H. Wildenthal, Michigan State University annual report, **1982–1983**, p. 78 (unpublished).

[27] G. Jakob, N. Benczer-Koller, G. Kumbartzki, J. Holden, T. J. Mertzimekis, K.-H. Speidel, R. Ernst, A. E. Stuchbery, A. Pakou, P. Maier-Komor, A. Macchiavelli, M. McMahan, L. Phair, and I. Y. Lee, Phys. Rev. C **65**, 024316 (2002).